JOC The Journal of Organic Chemistry

Article

pubs.acs.org/joc

Electronic Effects of Ring Fusion and Alkyne Substitution on Acene Properties and Reactivity

Jingjing Zhang, Zachary C. Smith, and Samuel W. Thomas III*

Departmentof Chemistry, Tufts University, 62 Talbot Avenue, Medford, Massachusetts 02155, United States

Supporting Information

ABSTRACT: This paper describes the synthesis and systematic study of substituted acenes that have differences in conjugation both along their long axes (by the number of fused benzene or thiophene rings) and along their short axes (by the number of arylethynyl substituents). These acenes include what we believe to be the first reported examples of five new subclasses of substituted acenes. Systematic analyses of data obtained using absorbance and fluorescence spectroscopies, cyclic voltammetry, and DFT calculations reveal clear correlations between these common structural perturbations to acene structure and the key parameters, such as HOMO−LUMO gap, frontier molecular orbital energies, and reactivity with singlet oxygen.

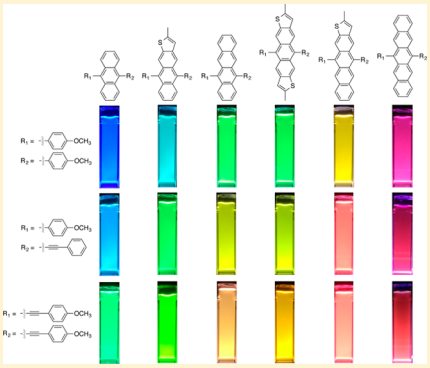

INTRODUCTION

Acenes are both a fundamentally important class of molecules in organic chemistry and frequently used components of organic electronic devices.[1−4] From anthracene as an early organic photoconductor[5] to current research on singlet fission for enhancing photon-to-electron conversion efficiency,[6] the photophysical, electrochemical, and transport properties of acenes such as tetracene, rubrene, and pentacene are key to their applications. Changes to the parent structures of acenes with either substituents or fused heteroaromatic rings have been important for tuning and improving the properties of acene-based materials. Some classes of examples include (1) aryl ring substituents for molecular switches or to induce steric hindrance,[7−13] (2) ethynylene or thiol substitution to improve the stability of large acenes to oxidation (this approach has enabled the isolation and characterization of stable derivatives of hexacene, heptacene, and nonacene),[14−20] (3) fused nitrogen- or sulfur-containing heteroaromatic rings for perturbing the properties of the acene,[21−23] and (4) halogenation or cyanation of acenes to create n-type materials.[24,25] Oligomers and polymers incorporating the structures of these acenes as repeating units are also finding increased popularity in the field.[26]

In addition to their physical properties, acenes also participate in rich cycloaddition chemistry.[27,28] Reactive dieneophiles such as maleimides[29−31] and benzynes[32,33] undergo [4 + 2] cycloaddition reactions with rings of the acene that are both electronically activated, those that yield the most aromatic stabilization upon reaction and have largest orbital coefficients, and sterically unencumbered.[34−36] A particularly important class of these reactions is the cycloaddition of singlet oxygen ($^1O_2$) with acenes to yield endoperoxides.[8,35,37,38] This reaction is a primary source of oxidative decomposition of acenes, particularly large acenes such as pentacene, with rate constants that can approach diffusion control.[14,39,40] $^1O_2$ is also a key reactive oxygen species in photodynamic therapy,[41] as well as a useful synthetic oxidant that is chemically amplifiable through photosensitization.[42,43] Endoperoxide formation is key to a number of luminescence-based $^1O_2$ sensing strategies, including those from our group.[44−52] Acene cycloaddition reactions have also been useful in photopatterning and imaging,[10,53] transducing signal in bioanalytical experiments,[54] and photochromic materials; tetracene was an early photochromic compound.[55]

With respect to structure−property relationships of these reactions, it is well-known that longer acenes generally undergo cycloaddition with $^1O_2$ faster than analogous shorter acenes. This trend breaks down, however, when comparing diethynyl-substituted pentacenes, with which $^1O_2$ reacts orders of magnitude more slowly than diethynyl tetracenes;[39,56] this is one of a number of features that makes diethynyl pentacenes promising for electronics applications.[16,25,57−59] Fudickar and Linker have determined that fast competitive physical quenching of $^1O_2$ by ethynyl-substituted pentacenes is key to their persistence.[39] In addition, both our group and the group of Linker have reported that ethynyl substitution lowers the activation energy of endoperoxide cycloreversion because of increased radical stabilization.[39,56,60]

Because of our group's interest in $^1O_2$-responsive luminescent materials, we have found it important to understand the relationship between chemical structures of substituted acenes and heteroacenes and their optical properties and reactivity with $^1O_2$, as well as be able to adjust acene structure to tune

Received: July 25, 2014
Published: October 22, 2014

   dx.doi.org/10.1021/jo501696d | J. Org. Chem. 2014, 79, 10081−10093

these properties. In pursuit of these goals, which we believe is shared by others for whom the properties and applications of acenes are important, this paper describes a systematic study of how these key properties, absorbance and photoluminescence behavior, frontier molecular orbital energies, and $^1O_2$ reactivity, depend on several important structural variables.

EXPERIMENTAL DESIGN

Based on previous work in which we and others have studied the effect of combinations of aryl and ethynyl substitution of tetracene and pentacene derivatives,[56,61,62] we targeted two structural features (Chart 1) that we reasoned would yield properties intermediate of more well understood structure–property relationships.

Chart 1. Acene Structural Perturbations Featured in This Work

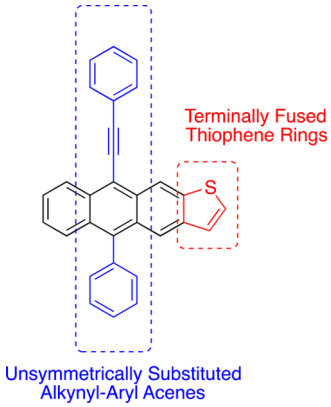

Unsymmetrically Substituted Aryl-Ethynyl Acenes. Many examples of symmetrically substituted diaryl and diethynyl acenes with more than three fused aromatic rings exist; they are often derived from addition of two equivalents of highly nucleophilic organometallic species, such as organolithium reagents, to quinones. Many examples of 9-aryl-10-ethynylanthracenes are also known, but longer acenes with analogous unsymmetric substitution patterns are comparatively rare: tetracene and pentacene dimers in this category exist,[63,64] and Tykwinski has described several 6-anthryl-13-ethynylpentacenes for use in field-effect transistors.[62] We recently reported sterically hindered 6-aryl-13-ethynylpentacenes with strong resistance to photooxidation.[61] Based on those studies, we suspected that aryl–ethynyl acenes with greater than three fused rings would show properties (HOMO–LUMO gap, reaction rates) between those of the analogous, symmetrically substituted diethynyl- and diarylacenes.

Acenes With Fused Terminal Thiophene Rings. This class of structures, such as anthradithiophenes and tetracenothiophenes,[65−67] are increasingly common design motifs in organic electronics.[23] The effect of these thiophene rings, however, on properties such as reactivity with $^1O_2$ in the continuum of carbocyclic acenes has not been characterized systematically to our knowledge. We hypothesized that because the resonance energy of thiophene (29 kcal/mol) is less than that of benzene (36 kcal/mol), properties of these molecules would be intermediate between those of fully carbocyclic acenes (i) with one fewer fused ring and (ii) with the same number of fused rings.

RESULTS AND DISCUSSION

Acene Synthesis. Scheme 1 summaries the synthetic approaches we took for the acenes described in this paper, all

Scheme 1. General Synthetic Approaches for Substituted Acenes

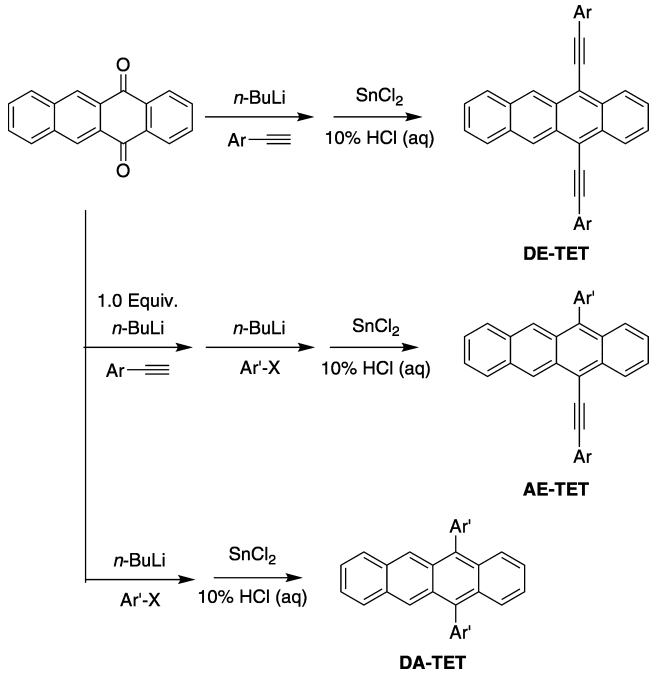

of which involved nucleophilic addition of appropriate organolithium reagents to the corresponding quinones followed by tin(II)-mediated reduction of the resulting diols to yield the target acene derivatives (Chart 2.) Aldol condensation reactions yielded those quinones that were not commercially available, as described in the literature.[68,69] Because of the strong Brønsted–Lowry basicity of aryllithium complexes, we prepared thienoacene derivatives substituted with methyl groups in the 2-positions of terminal fused thiophene rings; attempts to add aryllithium reagents to quinones that did not have these groups gave poor yields of products derived from deprotonation of terminal thiophene rings.[70] The synthesis of these methylated quinone starting materials for thienoacene derivatives is described in the Experimental Section. Otherwise, our approaches to the preparation of symmetrically substituted diaryl (**DA**) derivatives and diethynyl (**DE**) are typical for their preparation. The substitution patterns we chose, with two methoxy groups on symmetrically substituted acenes and one on the unsymmetrically substituted acenes, derive from the structures of ether-based linkers we use to prepare conjugated polymers that respond to $^1O_2$.[51]

For the unsymmetrical aryl–ethynyl (**AE**) acenes, our procedure was based on publications from Tykwinski and coworkers, using slow addition of 1 equiv of alkynyllithium to the quinone and isolating the resulting γ-hydroxyketone, followed by addition of an excess of aryllithium reagent, and finally reduction with $SnCl_2$ in aqueous acid. Tykwinski and coworkers have demonstrated that this approach is useful for preparing unsymmetric diethynylpentacenes.[71−73] Here we show that this approach is amenable to the preparation of unsymmetric arylethynyl derivatives of tetracene (**TET**), anthrathiophene (**AMT**), anthradithiophene (**ADT**), and

dx.doi.org/10.1021/jo501696d | J. Org. Chem. 2014, 79, 10081−10093

Chart 2. Structures and Acronyms for the Acenes Discussed in This Paper[a]

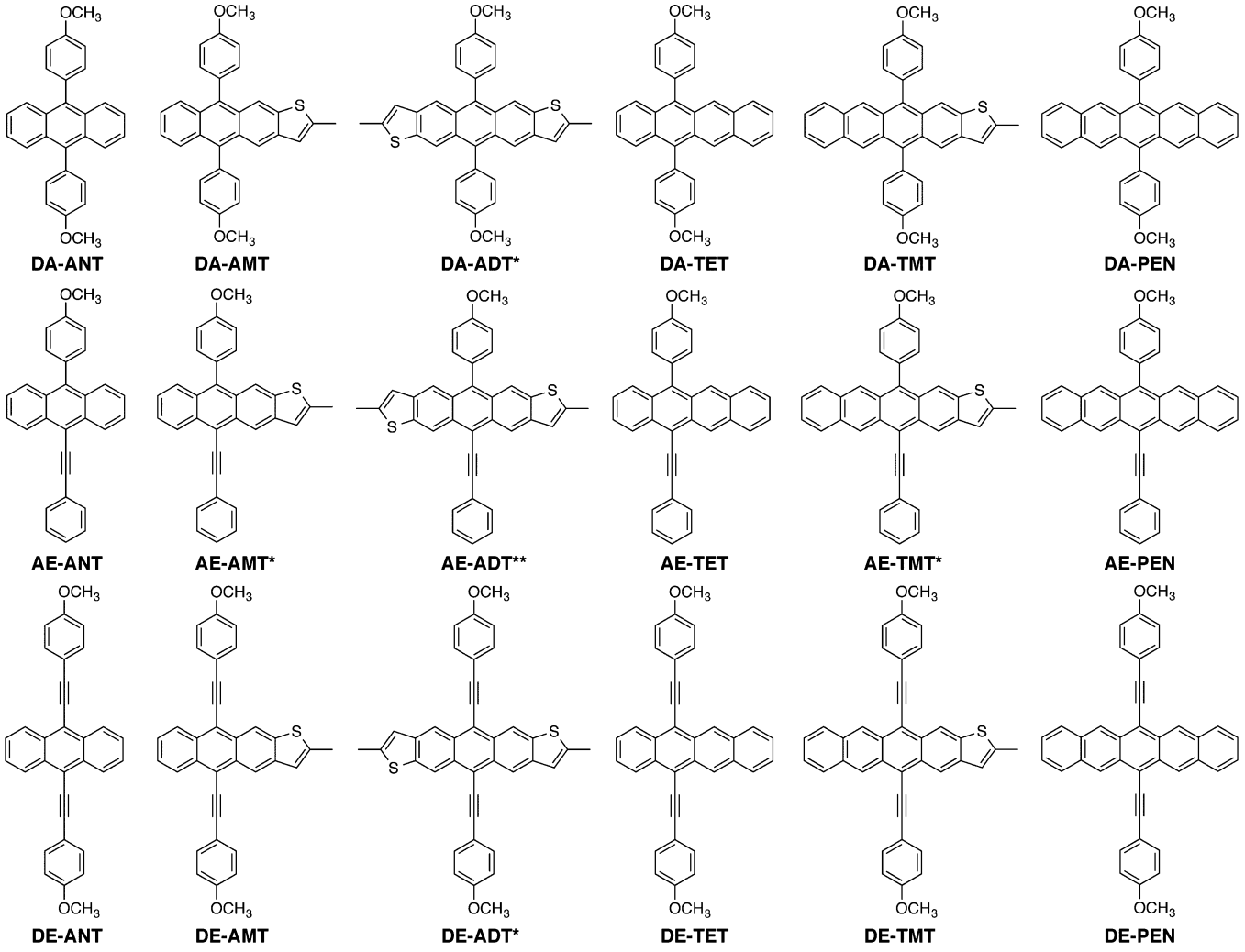

[a]Those labeled with * are isolated as mixtures of two isomers; **AE-ADT** (**) was isolated as three isomers.

Table 1. Solution-State Photophysical Parameters of Acenes in CH_2Cl_2

compound	$\lambda_{onset,abs}$,[a] nm (eV)	$\lambda_{max,abs}$ (nm)	ε (M^{-1} cm^{-1})	$\lambda_{max,fl}$ (nm)	Φ_f	τ (ns)
DA-ANT	420 (2.95)	376,[b] 263	12000	427	0.59	4.4
AE-ANT	455 (2.72)	411,[b] 308, 269	21000	452	0.51	2.8
DE-ANT	495 (2.50)	473,[b] 319, 276	42000	492	0.66	2.9
DA-AMT	472 (2.63)	450,[b] 291	10000	469	0.52	7.4
AE-AMT	533 (2.33)	481,[b] 333, 293	13800	504	0.73	7.1
DE-AMT	545 (2.27)	520,[b] 342, 294	36500	538	0.75	5.3
DA-ADT	520 (2.38)	500,[b] 308	11900	514	0.61	9.7
AE-ADT	584 (2.13)	539,[b] 334, 307	14000	561	0.71	10.8
DE-ADT	600 (2.07)	573,[b] 355, 310	39500	590	0.92	7.7
DA-TET	515 (2.41)	495,[b] 286	8800	511	0.64	12.1
AE-TET	553 (2.24)	523,[b] 338, 289	16600	550	0.60	9.7
DE-TET	585 (2.12)	559,[b] 359, 293	33100	576	0.85	7.0
DA-TMT	575 (2.16)	550,[b] 309	7600	570	0.55	15.4
AE-TMT	627 (1.98)	580,[b] 341, 312	6800	620	0.45	11.6
DE-TMT	650 (1.91)	615,[b] 369, 314	13600	634	0.64	11.8
DA-PEN	630 (1.97)	602,[b] 308	12700	620	0.09	7.8
AE-PEN	684 (1.81)	635,[b] 357, 311	9400	697	0.02	2.2
DE-PEN	705 (1.76)	666,[b] 377, 312	27300	706	0.03	4.6

[a]Estimated by the intersection of linear approximations of the red edge of the absorbance spectrum and the baseline at long wavelengths. [b]Wavelength at which extinction coefficient was reported.

dx.doi.org/10.1021/jo501696d | J. Org. Chem. 2014, 79, 10081−10093

tetracenothiophene (**TMT**). To the best of our knowledge, we are aware of no previously reported **AMT**, **ADT**, **TET**, or **TMT** derivatives with the unsymmetric aryl/ethynyl substitution patterns in the **AE** derivatives reported here, nor are we aware of any reported diaryl derivatives of the **TMT** core.

Substituted thienoacenes are often isolated and studied as isomeric mixtures because of the unsymmetric nature of the thiophene ring. Although different isolated isomers can differ in solid-state behavior such as crystal structure and device performance, they have nearly identical solution-state behavior, including UV/vis and electrochemistry, which makes their individual characterization here unnecessary.[74−76] **AE-AMT** and **AE-TMT** were therefore isolated as mixtures of the two possible isomers depending on whether the aryl ring was on the same or opposite side of the acene long axis as the sulfur atom, as indicated by the chemical shift of the β-protons on the fused thiophene rings (~6.9 or ~7.1 ppm), while **DA-ADT** and **DE-ADT** were isolated as mixtures of isomers regarding whether the sulfur atoms were on the same or opposite sides of the acene. Compound **AE-ADT** was isolated as a mixture of the three possible isomers resulting from a combination of these two structural variables.

Electronic Absorbance Spectra. We characterized each acene by electronic absorbance spectrophotometry and fluorescence spectroscopy in CH_2Cl_2; Table 1 summarizes the results of these experiments, grouped by the structure of the acene backbone, while Figure 1 displays the UV/vis spectra of acenes in CH_2Cl_2, grouped by the substitution pattern (**DA**, **AE**, or **DE**) of the acenes. All the spectra acquired share several features: each has both a sharp, intense absorbance band in the ultraviolet region of the spectrum and a lower energy band that shows a series of vibronic transitions characteristic of linear acenes, with differences between vibronic transitions ranging from 1200−1400 cm^{-1}.[20] UV/vis spectra of diaryl (**DA**) acene derivatives had better resolved vibronic intensity patterns; we attribute the broadening of **AE** and **DE** derivatives to the low rotation barriers of arylethynyl groups enabling a larger variety of accessible conformations with different excitation energies. The extinction coefficients of the long-wavelength bands of these compounds are typical of substituted acenes, with an approximate range of 5000 to 40000 M^{-1} cm^{-1}, with diethynyl substitution consistently yielding the largest values for each class of acene backbone.

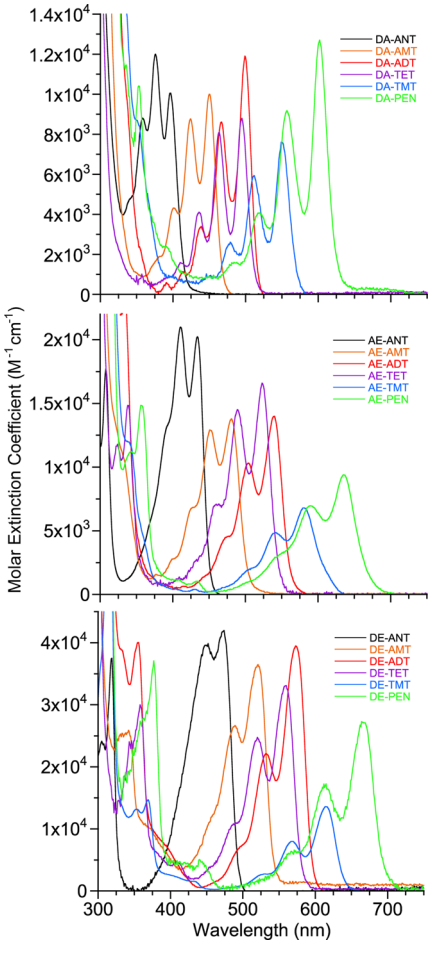

Figure 1. UV/vis absorbance spectra of all acenes in dichloromethane.

The second trend involves the dependence of HOMO−LUMO gap on the acene backbone: addition of a terminally fused thiophene ring to a fully carbocyclic acene backbone decreases the HOMO−LUMO gap by 50−60% of the decrease in HOMO−LUMO gap that results from addition of an additional benzene ring. For example, the ΔE_g for **DA-TET** and **DA-TMT** (addition of a fused thiophene ring to diaryltetracene) is −0.25 eV, while ΔE_g for **DA-TET** and **DA-PEN** (addition of a fused benzene ring to diaryl tetracene) is −0.44 eV. A second fused thiophene ring (comparing derivatives of **AMT** and **ADT**) yields a further red shift for these five-ring systems, such that analogously substituted anthradithiophenes and tetracenes have optical HOMO−LUMO gaps that are close in magnitude; they differ by less than 100 mV in the derivatives studied in this work. These results are consistent with the aromatic stabilization and extent of delocalization of a fused thiophene ring being smaller than a fused benzene ring and offer another, structurally orthogonal variable to the pattern of ethynyl or aryl substitution, for controlling the HOMO−LUMO gaps of these molecules.

Fluorescence Spectra. The luminescence properties of substituted acenes are critical for their use in sensing and solid-state lighting applications. Optimization of materials for these applications often requires tuning of emission color, efficiency, and rate. The development of approaches to modifying chemical structure to achieve desired luminescence properties is therefore an important goal. As summarized in Table 1, nearly all the substituted acenes investigated were efficient fluorophores with quantum yields of fluorescence (Φ_f) for most derivatives greater than 0.5. Only the pentacene derivatives were weakly luminescent, which we in part attribute to their low HOMO−LUMO gaps and therefore increased rate of nonradiative decay as we observed by time-resolved fluorescence. Also, the shapes of all fluorescence emission spectra were similar, with each spectrum showing vibronic resolution at ambient temperature in dichloromethane.

In addition, several readily identifiable trends relating acene structure to luminescence spectra exist that mirror those found in absorbance spectra. First, the trend in wavelengths of fluorescence maxima for compounds with a particular acene backbone increases in the order **DA** < **AE** < **DE** (Figure 2). This trend is analogous to the order of absorbance onset and is attributable to arylethynyl substituents contributing greater electronic delocalization than twisted aryl substituents. Second, as was the case with absorbance spectra, addition of a fused thiophene ring to a fully carbocyclic acene backbone yields a fluorescence spectrum red-shifted to a smaller degree than

dx.doi.org/10.1021/jo501696d | J. Org. Chem. 2014, 79, 10081−10093

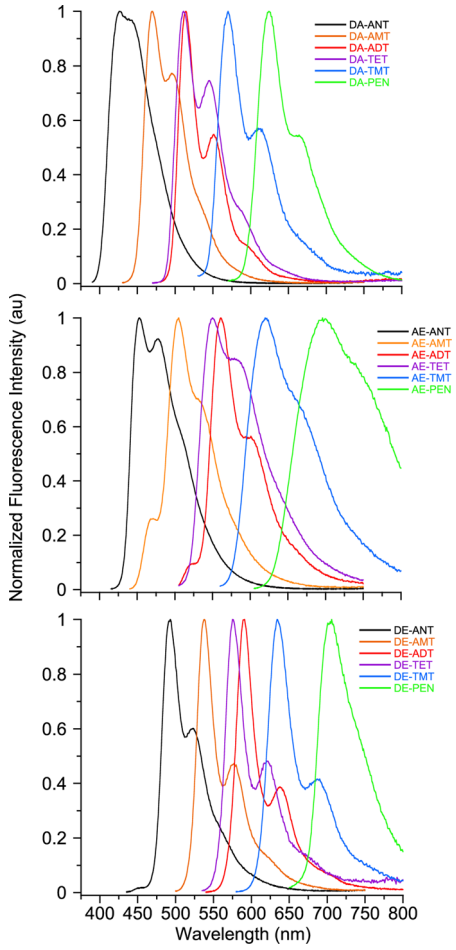

Figure 2. Height-normalized fluorescence emission spectra of all acenes in dichloromethane.

addition of a fused benzene ring. For example, the fluorescence emission maxima of **DA-TET**, **DA-TMT**, and **DA-PEN** are 511, 570, and 620 nm, respectively. Finally, addition of two fused terminal thiophene rings yields fluorescence spectra similar to the addition of one fused benzene ring: 14 nm (equivalent to 50 meV) was the largest observed difference between fluorescence maxima of analogously substituted **TET** and **ADT** derivatives. Noteworthy in these results is that the combination of a series of easily accessible acene backbones together with readily introduced aryl or ethynyl substituents generates compounds with emission spectra that both span the entire visible range of wavelengths and offer capability to tune emission color with fine control, all using the same general synthetic strategies and protocols.

Electrochemistry and DFT Calculations. We examined the effects of the structural perturbations on the frontier molecular orbital energies of these acenes, which we determined by two methods: (i) DFT calculations of each geometry-optimized acene using the B3LYP functional and 6-311G+(d,p) basis set with a polarizable dielectric continuum model for CH_2Cl_2 and (ii) cyclic voltammetry (CV) in deoxygenated CH_2Cl_2, using 0.1 M tetrabutylammonium hexafluorophosphate as the electrolyte at room temperature. Experimentally, we were able to determine the HOMO and LUMO energies of most derivatives by CV, as the average of cathodic and anodic peak potentials for the first oxidation and reduction waves of the neutral acenes; several compounds showed multiple waves at either positive or negative potential. For those molecules that did not show a readily assigned reduction wave in our CV experiments, we estimated LUMO energies by adding the optical HOMO–LUMO gap energy to the HOMO energy determined electrochemically. As shown in Table 2, the results of DFT calculations for the HOMO energies closely reproduced the experimental results, with differences no more than 0.11 eV. LUMO energies from the results of DFT calculations, however, were consistently smaller in magnitude, by as much as 0.36 eV, than those we measured

Table 2. HOMO and LUMO Energies of Acenes, Relative Observed Rates for Reactions of Acene with Photosensitized $^1O_2$, and Summary of the Calculated Triplet Energies of TMTs and PENs

	HOMO (eV)		LUMO (eV)			
compound	experiment	theory	experiment	theory	k_{rel}	triplet energy (calcd, eV)
DA-ANT	−5.56[39]	−5.57	−2.44[39]	−2.12	0.061 ± 0.01	
AE-ANT	*a*	−5.50	*a*	−2.48	0.014 ± 0.002	
DE-ANT	−5.30[39]	−5.24	−2.80[39]	−2.68	0.015 ± 0.003	
DA-AMT	−5.19	−5.26	−2.56	−2.20	0.25 ± 0.014	
AE-AMT	−5.24	−5.25	−2.71	−2.53	0.079 ± 0.008	
DE-AMT	−5.17	−5.09	−2.92	−2.71	0.023 ± 0.005	
DA-TET	−5.31	−5.22	−2.75	−2.52	1.0	
AE-TET	−5.23	−5.22	−2.93	−2.78	0.49 ± 0.13	
DE-TET	−5.17	−5.06	−3.10	−2.92	0.30 ± 0.09	
DA-ADT	−5.02	−5.03	−2.64	−2.28	0.97 ± 0.13	
AE-ADT	−5.03	−5.06	−2.76	−2.57	0.47 ± 0.11	
DE-ADT	−4.99	−4.94	−2.98	−2.75	0.12 ± 0.008	
DA-TMT	−4.98	−5.00	−2.76	−2.57	6.4 ± 0.55	1.23
AE-TMT	−5.04	−5.02	−2.96	−2.81	3.0 ± 0.76	1.10
DE-TMT	−4.99	−4.91	−3.14	−2.95	0.27 ± 0.14	0.95
DA-PEN	−4.98	−4.96	−2.96	−2.82	10.5 ± 0.04	0.96
AE-PEN	−5.03	−4.93	−3.15	−2.96	1.3 ± 0.16	1.00
DE-PEN	−4.99	−4.88	−3.31	−3.13	0.011 ± 0.002	0.74

[a]Not measured.

dx.doi.org/10.1021/jo501696d | J. Org. Chem. 2014, 79, 10081−10093

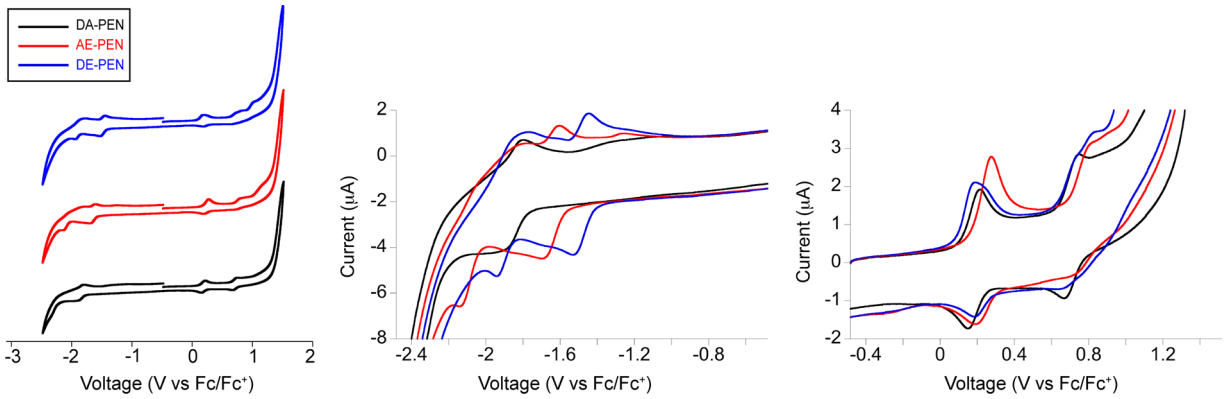

Figure 3. Cyclic voltammograms of the three **PEN** derivatives in deoxygenated CH_2Cl_2 at room temperature. The reduction potentials of the acenes (middle) depend strongly on whether the substituents are aryl or alkynyl groups; the oxidation potentials of the acenes (right), however, show a significantly smaller dependence.

electrochemically, a trend that Miller and co-workers also noted in their study of substituted pentacenes.[12] Nevertheless, although the magnitudes of calculated LUMO energies are systematically skewed relative to experimental values, the trends in calculated LUMO energies reproduce those observed experimentally.

As shown in Table 2 and Figure 3, extension of conjugation along the short axis by substituting arylethynyl substituents for aryl substituents leads to significant lowering of the FMO gap in both the homoacenes and the heteroacenes. Both our experimental and theoretical results indicate that significant decrease in LUMO energies with additional arylethynyl groups is the cause of this trend. As an example, Figure 3 shows cyclic voltammograms for the three substituted pentacene derivatives: while the three oxidation waves occur within ~100 mV of each other, the reduction waves show a clear trend with the magnitudes of reduction potentials increasing in the order **DE-PEN** < **AE-PEN** < **DA-PEN**. Outside of the anthracene derivatives, the largest deviation in HOMO energies among the acenes sharing identical backbones was less than 0.14 eV, between **DA-TET** and **DE-TET**, while the LUMO energies differ in a range from 0.34 to 0.38 eV. This general trend, which we observe in all these series of compounds, is consistent with trends reported in previous studies of pentacene derivatives.[8,10,12,15,40,77] Figure 4 shows an example of this general trend with **TMT** derivatives.

Fusing additional thiophene or benzene rings to the acenes extends their conjugation along the long axis of the acene core and leads to a reduction in HOMO−LUMO gap as demonstrated in the absorbance and fluorescence spectra displayed in Figures 1 and 2. Results from Table 2 and Figure 4 illustrate the differing effects of fusion of additional thiophene or benzene rings. Benzene ring fusion (comparing either **ANT**, **TET**, and **PEN** derivatives or **AMT** and **TMT** derivatives) results in both significant increases in HOMO energies (ΔE = 0.22 ± 0.04 eV) and decreases in LUMO energies (ΔE = −0.24 ± 0.04 eV). In strong contrast, most of the reduction in HOMO−LUMO gap from fusion of a terminal thiophene ring (comparing either **ANT**, **AMT**, and **ADT** derivatives or **TET** and **TMT** derivatives) derives from increases in HOMO energies (ΔE = 0.22 ± 0.08 eV), while decreases in LUMO energies are significantly smaller (ΔE = −0.06 ± 0.04 eV). This general trend is similar to that observed in a study comparing diethynylated pentacenes to either analogous anthradithiophene or tetracenothiophene derivatives.[78,79]

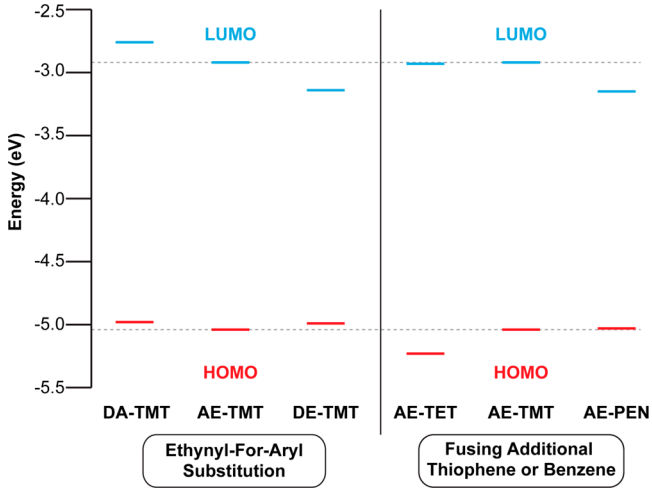

Figure 4. Energies of electrochemically determined frontier molecular orbitals of some acene derivatives showing the effects of (i) replacing aryl substituents with arylethynyl substituents and (ii) fusing a terminal thiophene or benzene ring onto the acene core.

Reactivity with $^1O_2$ Generated by Photosensitization. The reaction of acenes with $^1O_2$ to form endoperoxides is a primary path for the photochemical decomposition of acenes (type II photooxidation). In the photodecomposition of acenes, the acene generally serves as a photosensitizer by donating energy from its excited state to ground-state O_2 to generate $^1O_2$, which can then undergo [4 + 2] cycloaddition with an acene to yield an endoperoxide. Other established photochemical decomposition pathways of acenes are type I photooxidations that proceed via electron transfer and [4 + 4] "butterfly" dimerizations. To understand how the modifications to acene structure described above affect their reactivity with $^1O_2$, we examined the kinetics of acene disappearance upon exposure to $^1O_2$ generated by photosensitization using the sensitizer methylene blue (MB, Figure 5).

An important difference between this approach and a frequently used alternative, monitoring the rate of acene disappearance upon direct irradiation of the acene, is that the amount of light absorbed by the sensitizer (and therefore the rate of generation of $^1O_2$) can usually be controlled to be the same in each experiment. Experiments in which direct irradiation of the acene causes decomposition yield numerous

dx.doi.org/10.1021/jo501696d | J. Org. Chem. 2014, 79, 10081−10093

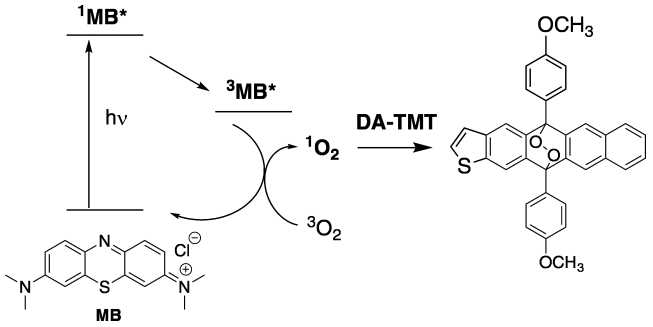

Figure 5. Process of endoperoxidation of an example acene (**DA-TMT**) using methylene blue (**MB**) as a singlet oxygen photosensitizer.

differences between acenes besides the rate of the bimolecular reaction between $^1O_2$ and acene: how the spectrum of the irradiation source overlaps with the absorbance spectrum of different acenes, the differences in excited state lifetime and quantum yields of acene-sensitized $^1O_2$ production, and the influence of acene photodimerization. Therefore, although experiments that measure decomposition upon direct acene irradiation are important since they more accurately mimic operational conditions in devices, in these studies we used a separate sensitizer that can in most cases be irradiated selectively with red light to have a clear correlation of $^1O_2$–acene reactivity and chemical structure. In those circumstances in which selective irradiation of MB is not possible because of overlap of the absorption spectra of MB and the acene (**AE-PEN** and **DE-PEN**), we ensured that the concentrations of the acene and MB were such that >90% of the incident light was absorbed by MB. Figure 6 shows examples of the changes to electronic absorbance spectra of the **AMT** derivatives during exposure to photosensitized $^1O_2$, as well as examples of the change in concentration of acene as a function of irradiation time and fits of these data to pseudo-first-order kinetics; the Supporting Information contains analogous data for all other acenes pictured in Chart 2. Table 2 and Figure 7 summarize the

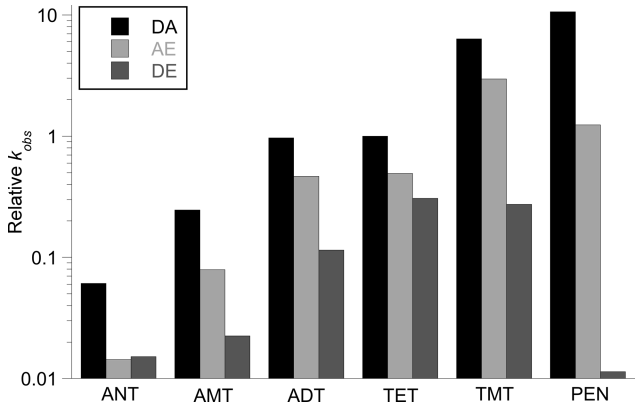

Figure 7. Dependence of observed rate of acene photooxidation during exposure to photosensitized $^1O_2$ on acene chemical structure.

observed relative rate constants, k_{rel}, of $^1O_2$–acene cycloaddition for each acene in Chart 2 (the observed rate for **DA-TET** is set at 1). We examined how (i) addition of fused aromatic rings and (ii) substitution of ethynyl for aryl groups affected acene photooxidative reactivity. Longer acenes, which contain more linearly fused rings in the backbone, generally have overall higher reactivity in cycloaddition reactions, including those with $^1O_2$, than shorter acenes, due to decreasing aromatic stabilization for each ring. We observed this trend with both the well-known fully carbocyclic acenes and the thienoacenes shown in Chart 2. Because both the FMO energy gaps of acenes and their observed rate of reaction with $^1O_2$ depend on the length of acene, there is a clear correlation between FMO energy gap and reaction rate for acenes with the same substitution pattern, **DA**, **AE**, or **DE** (Figure 2). The exceptions to this trend are the ethynylated pentacene derivatives and **DE-TMT**.[39]

The effect of increasing conjugation along the acene short axis by incorporating arylethynyl groups is to decrease $^1O_2$ reactivity from **DA**- to **AE**- to **DE**-derivatives among either the

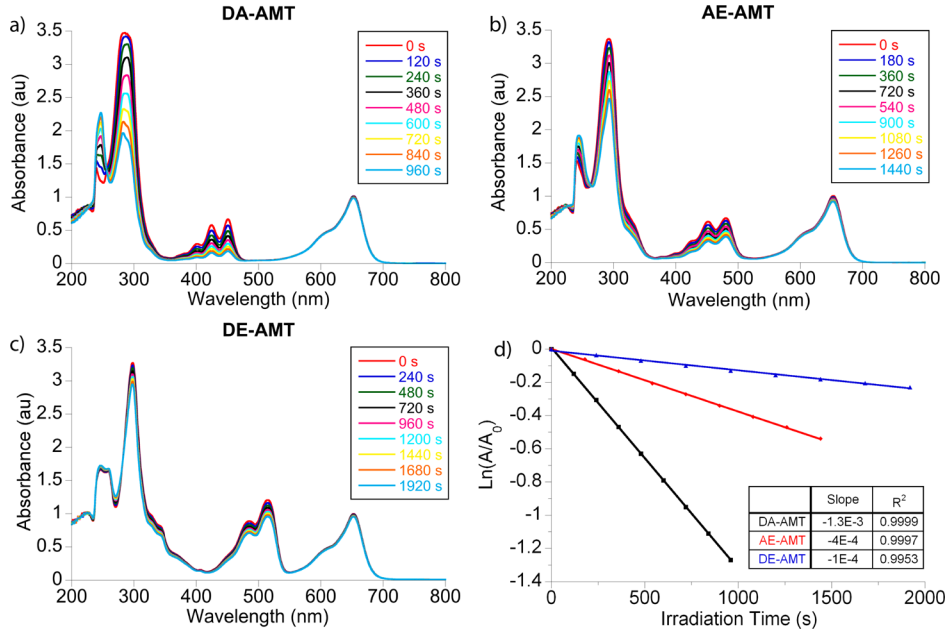

Figure 6. UV/vis response of **DA-AMT** (a), **AE-AMT** (b), and **DE-AMT** (c) to $^1O_2$ photosensitization with methylene blue (λ_{max} = 654 nm) in $CHCl_3$ and (d) pseudo-first order kinetics of reaction of **DA-AMT**, **AE-AMT**, and **DE-AMT** under these conditions.

dx.doi.org/10.1021/jo501696d | J. Org. Chem. 2014, 79, 10081–10093

homoacenes or the heteroacenes. These changes in substitution, however, do not yield significant changes in the energies of HOMOs (*vide supra*). Therefore, we conclude, as Fudikar and Linker recently noted with tetracenes and anthracenes, that the oxidation potential of these acenes is not a key factor in their reactivity with $^1O_2$.[39] Instead, the results reported here are consistent with the conclusion of Fudikar and Linker, who proposed a competition in the mechanism of the addition of $^1O_2$ to acenes between concerted and stepwise mechanisms.[39] Unlike aryl substituents, the phenylethynyl substituents do not stabilize zwitterionic intermediates effectively, resulting in phenylethynyl-substituted acenes favoring a concerted mechanism, resulting in the observed reduction in reaction rates with $^1O_2$.

Competitive cycloreversion of endoperoxides is another factor that impacts the observed rate of photooxidation of **DE-ANT** and **DE-AMT**. It is known that endoperoxides of 9,10-diethynylanthracenes reconvert to anthracenes rapidly in solution at room temperature, with half-lives on the order of 15−30 min, because of the stabilization of biradical intermediates of homolytic C−O bond cleavage.[39,60] In agreement with this observation, we found that upon photooxidation of **DE-AMT**, which has one thiophene ring fused onto the anthracene core, regeneration of the acene occurs at room temperature at a rate that contributes to the observed rate of photooxidation (see Supporting Information). No other compounds, including any of the investigated monoethynylated **AE** derivatives, showed any significant regeneration of acene on the time scale of the photolysis experiments (40 min).

Finally, it is noteworthy that $^1O_2$-reactivity of **DE-PEN** is about 3 orders of magnitude smaller than that of **DA-PEN**, while the corresponding decrease ranges from 3 to 20 times from **DA** to **DE** derivatives for the other acenes. Low energy LUMOs are reported to be important to the extraordinary persistence of diethynylpentacenes under photooxidative conditions;[40] as shown in Table 2, **DE-PEN** indeed has the lowest energy LUMO of all compounds investigated. Given that we are using an external photosensitizer, however, either an inhibition of photoinduced electron transfer from excited **DE-PEN** to O_2 or prevention or slow $^1O_2$ sensitization from excited **DE-PEN** seems unlikely to be the cause of the persistence of **DE-PEN** in these particular experiments. Fudickar and Linker attributed this extraordinary persistence under external photosensitization to physical quenching of $^1O_2$ based on an elegant experiment, in which the presence of **DE-PEN** inhibited the $^1O_2$-induced oxidation of a more reactive acene.[39] We further investigated the possibility that energy transfer from $^1O_2$ to **DE-PEN** is a mechanism for physical deactivation of $^1O_2$ by calculating the triplet energies of several acenes using the B3LYP functional and the Tamm−Dancoff approximation, which is known to show increased accuracy in calculating the low-energy excited states of linear acenes, particularly triplet states.[80] The symmetrically substituted **DE-PEN** has a calculated triplet energy (0.74 eV) significantly lower than any other acene investigated in this work or the energy of singlet oxygen (~0.97 eV), indicating that physical quenching by energy transfer (eq 1) from $O_2(^1\Delta_g)$ to **DE-PEN** would be exergonic. This mechanism of quenching of $^1O_2$ would be similar to the quenching of $O_2(^1\Delta_g)$ by other molecules with low triplet energies such as carotenoids (~0.88 eV).[81,82]

$$O_2(^1\Delta_g) + S_0 \rightarrow O_2(^3\Sigma_g^-) + T_1 \quad (1)$$

CONCLUSION

Work described in this paper has focused on a thorough study of the effects of common approaches to increasing electronic delocalization in acenes, fusion of benzene or terminal thiophene rings to the acene core, as well as substitution of ethynyl substituents for aryl substituents, on key properties. As part of this study, we have prepared five previously unreported subclasses of substituted acenes and thienoacenes, including several derivatives that are unsymmetrically substituted about the acene long axis. Beyond the new compounds reported, an important conclusion from this work is how different structural perturbations to acene structure affect unimolecular physical properties in solution. Through both theoretical and experimental evidence, we showed that bathochromic shifts in HOMO−LUMO gaps for the structural perturbations of (i) monoethynylation or (ii) thiophene ring fusion were smaller than (i) diethynylation or (ii) benzene ring fusion, as to be expected based on the extent of increasing the degree of conjugation. The reasons for these bathochromic shifts, however, are different for the two types of substitution: extending conjugation along the acene short axis with ethynyl substitution resulted primarily in a lowering of LUMO energy, while thiophene ring fusion along the acene long axis resulted primarily in an increase of HOMO energy. These structure−property relationships make properties such as fluorescence color and redox potentials of acenes increasingly predictable and tunable.

Additional conclusions concern structure−property relationships of acene photo-oxidation. The observed rate of photo-oxidative decomposition generally conforms to the trend that additional fused aromatic rings yield increasingly reactive derivatives, with fused thiophene rings, which have smaller resonance energy, yielding smaller increases in reactivity than the same number of fused benzene rings. In addition, this work highlights several approaches to increasing the resistance to photooxidative decomposition. Acenes that form endoperoxides across ethynylated positions can undergo cycloreversion reactions,[60] with short acenes such as **DE-ANT** and **DE-AMT** doing so at room temperature. Acenes with low triplet energies, such as **DE-PEN**, can also resist decomposition by physically quenching $^1O_2$.[39] Taking only this approach, however, probably has a limited structural range with respect to acene length, since it is known that ethynylated hexacenes decompose by dimerization through alkyne−acene cycloaddition.[19] Steric inhibition of cycloaddition reactions, achieved through both bulky silylethynyl groups and aryl substituents, also increases the persistence of acene derivatives in solution.[14,20,61,83] We believe that the systematic and broad nature of this study will be useful for researchers whose goals include designing or modifying acenes to target specific combinations of properties.

EXPERIMENTAL SECTION

General Information. All synthetic manipulations were performed under standard air-free conditions under an atmosphere of argon gas with magnetic stirring unless otherwise mentioned. Flash chromatography was performed using silica gel (230−400 mesh) as the stationary phase. NMR spectra were acquired on a 500 MHz spectrometer. Chemical shifts are reported relative to residual protonated solvent (7.27 ppm for $CHCl_3$). High-resolution mass spectra (HRMS) were obtained using a Fourier transform ion cyclotron resonance mass spectrometer and a peak-matching protocol to determine the mass and error range of the molecular ion. 9,10-Bis(4-methoxyphenyl)-anthracene (**DA-ANT**),[8] 9,10-bis((4-methoxy-phenyl)ethynyl)-anthracene (**DE-ANT**),[60] 5,12-bis(4-methoxyphenyl)tetracene (**DA-**

dx.doi.org/10.1021/jo501696d | J. Org. Chem. 2014, 79, 10081−10093

TET),[51] 5,12-bis((4-methoxy-phenyl)ethynyl)tetracene (**DE-TET**),[56] 6,13-bis(4-methoxyphenyl)pentacene (**DA-PEN**),[56] 6,13-bis((4-methoxy-phenyl)ethynyl)pentacene (**DE-PEN**),[56] 5-methylthiophene-2,3-dicarbaldehyde,[84] and 2,8-dimethyl-anthra[2,3-*b*:6,7-*b*′]-dithiophene-5,11-dione (**ADT quinone**)[80] were prepared as previously reported.

Electronic absorbance spectra were acquired with a spectrophotometer in double-beam mode using a solvent-containing cuvette for background subtraction spectra. Fluorescence spectra were collected at a 90° angle from the incident irradiation and corrected for both fluctuations in the lamp intensity and the wavelength-dependent sensitivity of the photomultiplier tube. Fluorescence quantum yields were determined relative to either (i) quinine sulfate in 0.1 M H_2SO_4[85] (all **ANT** derivatives), (ii) coumarin 6 in ethanol[86] (**DA-TET**, **AE-TET**, **DA-AMT**, **AE-AMT**, and **DA-ADT**), (iii) rhodamine 6G in ethanol[85] (**AE-ADT** and **DE-AMT**), or (iv) cresyl violet in methanol[85] (**DE-TET**, **DE-ADT**, and all **TMT** and **PEN** derivatives). Time-resolved fluorescence data was collected using a time-correlated single-photon counting instrument with a pulsed LED operating at 403 nm. Cyclic voltammograms were acquired using a three-electrode setup with platinum working and counter electrodes and a Ag/AgCl reference electrode and are reported relative to the ferrocene/ferrocenium redox couple measured as an external standard under identical conditions. Irradiation of the methylene blue photosensitizer to generate $^1O_2$ was performed with a 200 W Hg/Xe lamp equipped with a condensing lens, water filter, and manual shutter, with a 400 nm high-pass filter, a 665 nm high-pass filter, and a focusing plano-convex lens (focal length 15 cm) in the light path. DFT calculations were performed using the Gaussian 09 software package,[87] with optimized geometries and FMO energies determined at the B3LYP/6-31G**(d,p) level of theory using a polarizable continuum solvent model for CH_2Cl_2. Triplet energies of these optimized geometries were calculated with the same functional and basis set, using the Tamm−Dancoff approximation.

9-(4-Methoxyphenyl)-10-(phenylethynyl)-anthracene (AE-ANT). *n*-Butyllithium (0.60 mL, 0.96 mmol, 1.6 M) in hexanes was added to solution of 0.12 mL (1.06 mmol) phenylacetylene in 2 mL of dry THF slowly at −78 °C, and the mixture was stirred vigorously for 45 min. The reaction mixture was slowly added to a solution of 0.20 g (0.96 mmol) of anthracene-9,10-dione in 3 mL of dry THF at −78 °C. The solution was then allowed to slowly warm to room temperature and stirred overnight. The reaction mixture was filtered, and the solid in the filter was washed with 10 mL of THF/H_2O (1:1, v/v). The filtrate was mixed with NH_4Cl saturated aqueous solution, and the mixture was vigorously stirred for 30 min. The suspension was then extracted with CH_2Cl_2 and dried over $MgSO_4$. The crude 10-hydroxy-10-(phenylethynyl)-anthracen-9(10*H*)-one was used without further purification.

n-Butyllithium (0.92 mL, 1.5 mmol, 1.6 M) in hexanes was added to a solution of 0.19 mL (1.5 mmol) of 4-methoxybromobenzene in 2 mL of dry THF, and the mixture was stirred vigorously for 1 h. 10-Hydroxy-10-(phenylethynyl)-anthracen-9(10*H*)-one (0.12 g, 0.39 mmol) was dissolved in 3 mL of dry THF in a separate flask and cooled to −78 °C followed by the addition of the aryllithium suspension, and the reaction mixture was stirred overnight while slowly warming to room temperature. The reaction mixture was then treated with 20 mL of 10% HCl aqueous solution saturated with tin(II) chloride dihydrate and extracted with CH_2Cl_2 and dried over $MgSO_4$. The crude **AE-ANT** was purified by flash chromatography on silica gel using CH_2Cl_2/hexanes (1:2, v/v) and then recrystallized from CH_2Cl_2 and hexanes. **AE-ANT** (0.10 g, 69%). Mp: 238−240 °C. ^{1}H NMR (500 MHz, $CDCl_3$): δ 8.73 (d, J = 8.6 Hz, 2H), 7.80 (d, J = 7.0 Hz, 2H), 7.73 (d, J = 8.8 Hz, 2H), 7.60−7.57 (m, 2H), 7.48−7.45 (m, 2H), 7.43−7.38 (m, 3H), 7.36−7.34 (m, 2H), 7.13 (d, J = 8.6 Hz, 2H), 3.96 (s, 3H). ^{13}C NMR (125 MHz, $CDCl_3$): δ 159.3, 138.4, 132.5, 132.4, 131.8, 130.7, 130.4, 128.7, 128.6, 127.7, 127.1, 126.4, 125.7, 123.9, 117.4, 114.0, 101.0, 86.8, 55.6. HRMS (DART): calcd for $C_{29}H_{21}O$ (M + H)$^+$ 385.1587, found 385.1581.

5-(4-Methoxyphenyl)-12-(phenylethynyl)tetracene (AE-TET). *n*-Butyllithium (0.97 mL, 1.6 mmol, 1.6 M) in hexanes was added to solution of 0.21 mL (1.9 mmol) of phenylacetylene in 3.2 mL of dry THF slowly at −78 °C, and the mixture was stirred vigorously for 45 min. The reaction mixture was slowly added to a solution of 0.50 g (1.9 mmol) of tetracene-5,12-dione in 5.5 mL of dry THF at −78 °C. The solution was then allowed to slowly warm to room temperature and stirred overnight. The reaction mixture was filtered, and the solid in the filter was washed with 15 mL of THF/H_2O (1:1, v/v). The filtrate was mixed with NH_4Cl saturated aqueous solution, and the mixture was vigorously stirred for 30 min. The suspension was then extracted with CH_2Cl_2 and dried over $MgSO_4$. The crude 12-hydroxy-12-(phenylethynyl)tetracen-5(12*H*)-one was used without further purification.

n-Butyllithium (2.0 mL, 3.3 mmol, 1.6 M) in hexanes was added to a solution of 0.42 mL (3.3 mmol) of 4-methoxybromobenzene in 3 mL of dry THF, and the mixture was stirred vigorously for 1 h. 12-Hydroxy-12-(phenylethynyl)tetracen-5(12*H*)-one (0.30 g, 0.83 mmol) was dissolved in 4 mL of dry THF in a separate flask and cooled to −78 °C followed by the addition of the aryllithium suspension, and the reaction mixture was stirred overnight while slowly warming to room temperature. Then the reaction mixture was treated with 20 mL of 10% HCl aqueous solution saturated with tin(II) chloride dihydrate, extracted with CH_2Cl_2, and dried over $MgSO_4$. The crude **AE-TET** was purified by flash chromatography on silica gel using CH_2Cl_2/hexanes (1:2, v/v) and then recrystallized from CH_2Cl_2 and hexanes to yield **AE-TET** (0.21 g, 58%). Mp: 234−235.5 °C. ^{1}H NMR (500 MHz, $CDCl_3$): δ 9.36 (s, 1H), 8.74 (d, J = 8.8 Hz, 1H), 8.36 (s, 1H), 8.11 (d, J = 8.6 Hz, 1H), 7.88 (d, J = 7.3 Hz, 2H), 7.85 (d, J = 8.6 Hz, 1H), 7.74 (d, J = 8.9 Hz, 1H), 7.54−7.50 (m, 3H), 7.48−7.43 (m, 4H), 7.39−7.32 (m, 2H), 7.20 (d, J = 8.4 Hz, 2H), 4.01 (s, 3H). ^{13}C NMR (125 MHz, $CDCl_3$): δ 159.4, 138.5, 132.8, 132.6, 131.9, 131.8, 131.6, 130.9, 130.5, 129.9, 129.4, 128.7, 128.65, 128.55, 127.7, 127.2, 126.7, 126.4, 126.0, 125.54, 125.49, 125.3, 124.0, 117.1, 114.1, 101.9, 87.3, 55.6. HRMS (DART): calcd for $C_{33}H_{23}O$ (M + H)$^+$ 435.1743, found 435.1735.

6-(4-Methoxyphenyl)-13-(phenylethynyl)pentacene (AE-PEN). *n*-Butyllithium (0.79 mL, 1.3 mmol, 1.6 M) in hexanes was added to solution of 0.18 mL (1.6 mmol) of phenylacetylene in 3.2 mL of dry THF slowly at −78 °C, and the mixture was stirred vigorously for 45 min. The reaction mixture was slowly added to a solution of 0.50 g (1.6 mmol) of pentacene-6,13-dione in 5.5 mL of dry THF at −78 °C. The solution was then allowed to slowly warm to room temperature and stirred overnight. The reaction mixture was filtered, and the solid in the filter was washed with 15 mL of THF/H_2O (1:1, v/v). The filtrate was mixed with NH_4Cl saturated aqueous solution, and the mixture was vigorously stirred for 30 min. The suspension was then extracted with CH_2Cl_2 and dried over $MgSO_4$. The crude 13-hydroxy-13-(phenylethynyl)pentacen-6(13*H*)-one was used without further purification.

n-Butyllithium (0.91 mL, 1.5 mmol, 1.6 M) in hexanes was added to a solution of 0.19 mL (1.5 mmol) of 1-bromo-4-methoxybenzene in 3 mL of dry THF, and the mixture was stirred vigorously for 1 h. 13-Hydroxy-13-(phenylethynyl)pentacen-6(13*H*)-one (0.20 g, 0.49 mmol) was dissolved in 6 mL of dry THF in a separate flask and cooled to −78 °C followed by the addition of the aryllithium suspension, and the reaction mixture was stirred overnight while slowly warming to room temperature. Then the reaction mixture was treated with 20 mL of 10% HCl aqueous solution saturated with tin(II) chloride dihydrate, extracted with CH_2Cl_2, and dried over $MgSO_4$. The crude **AE-PEN** was purified by flash chromatography on silica gel using CH_2Cl_2/hexanes (1:2, v/v) and then recrystallized from CH_2Cl_2 and hexanes to yield **AE-PEN** (0.15 g, 63%). Mp: >260 °C. ^{1}H NMR (500 MHz, $CDCl_3$): δ 9.36 (s, 2H), 8.37 (s, 2H), 8.06 (d, J = 8.6 Hz, 2H), 7.95 (d, J = 7.1 Hz, 2H), 7.79 (d, J = 8.6 Hz, 2H), 7.57−7.49 (m, 6H), 7.39 (t, J = 7.3 Hz, 2H), 7.31 (t, J = 7.4 Hz, 2H), 7.25 (s, 1H), 4.06 (s, 3H). ^{13}C NMR (125 MHz, $CDCl_3$): δ 159.5, 138.5, 132.8, 132.0, 131.9, 131.5, 131.2, 130.8, 129.0, 128.83, 128.78, 128.7, 128.6, 126.6, 126.0, 125.5, 125.4, 124.1, 114.2, 103.0, 88.1, 55.6. HRMS (DART): calcd for $C_{37}H_{25}O$ (M + H)$^+$ 485.1900, found 485.1914.

2-Methylanthra[2,3-*b*]thiophene-5,10-dione (AMT quinone). 5-Methylthiophene-2,3-dicarbaldehyde (0.20 g, 1.3 mmol) and naphthalene-1,4-diol (0.21 g, 1.3 mmol) were dissolved in 3 mL of dry pyridine and heated at 120 °C for 24 h. After slow cooling to room temperature, the reaction mixture was filtered, and the solid in the filter was washed with 10 mL of deionized H_2O and 5 mL of acetone. The crude 2-methylanthra[2,3-*b*]thiophene-5,10-dione (0.34 g, 95%) was used without further purification. Mp: >260 °C. ^{1}H NMR (500 MHz, $CDCl_3$): δ 8.72 (s, 1H), 8.59 (s, 1H), 8.36−8.34 (m, 2H), 7.81−7.79 (m, 2H), 7.23 (m, 1H), 2.684, 2.681 (s, 3H). ^{13}C NMR (125 MHz, $CDCl_3$): δ 183.6, 183.2, 148.2, 145.2, 144.6, 134.30, 134.27, 134.22, 134.15, 130.1, 128.7, 127.5, 123.2, 122.25, 122.23, 16.8. HRMS (DART): calcd for $C_{17}H_{11}O_2S$ $(M + H)^+$ 279.0474, found 279.0467.

5,10-Bis(4-methoxyphenyl)-2-methylanthra[2,3-*b*]thiophene (DA-AMT). *n*-Butyllithium (0.68 mL, 1.1 mmol, 1.6 M) in hexanes was added to a solution of 0.14 mL (1.1 mmol) of 1-bromo-4-methoxybenzene in 4 mL of dry THF at −78 °C and stirred vigorously for 20 min, followed by the addition of 0.080 g (0.29 mmol) of **AMT quinone**. The reaction mixture was then allowed to slowly warm to room temperature overnight before addition of 20 mL of 10% HCl aqueous solution saturated with tin(II) chloride dihydrate and extracted with CH_2Cl_2. The crude product was purified by flash chromatography on silica gel (CH_2Cl_2/hexanes, 1:1, v/v) and recrystallized from CH_2Cl_2 and hexanes to yield **DA-AMT** (0.040 g, 32%). Mp: >260 °C. ^{1}H NMR (500 MHz, $CDCl_3$): δ 8.08 (s, 1H), 7.97 (s, 1H), 7.71−7.69 (m, 2H), 7.42 (d, J = 8.6 Hz, 4H), 7.28−7.26 (m, 2H), 7.17 (d, J = 8.0 Hz, 4H), 6.87 (s, 1H), 3.98 (s, 6H), 2.534, 2.532 (s, 3H). ^{13}C NMR (125 MHz, $CDCl_3$): δ 159.3, 159.2, 143.6, 140.0, 138.9, 136.8, 135.7, 132.8, 132.7, 131.8, 131.6, 129.8, 129.7, 129.0, 128.6, 127.2, 127.1, 124.65, 124.62, 121.2, 119.5, 119.1, 114.21, 114.16, 55.6, 17.0. HRMS (DART): calcd for $C_{31}H_{25}O_2S$ $(M + H)^+$ 461.1570, found 461.1569.

5-(4-Methoxyphenyl)-2-methyl-10-(phenylethynyl)anthrax-[2,3-*b*]thiophene (AE-AMT). *n*-Butyllithium (0.28 mL, 0.44 mmol, 1.6 M) in hexanes was added to a solution of 0.050 mL (0.47 mmol) of phenylacetylene in 2 mL of dry THF slowly at −78 °C, and the mixture was stirred vigorously for 45 min. The reaction mixture was slowly added to a solution of 0.13 g (0.47 mmol) of **AMT quinone** in 2 mL of dry THF at −78 °C. The solution was then allowed to slowly warm to room temperature and stirred overnight. The reaction mixture was filtered, and the solid in the filter was washed with 7 mL of THF/H_2O (1:1 v/v). The filtrate was mixed with NH_4Cl saturated aqueous solution and vigorously stirred for 30 min. The suspension was then extracted with CH_2Cl_2 and dried over $MgSO_4$. The crude 10-hydroxy-2-methyl-10-(phenylethynyl)anthra[2,3-*b*]thiophene-5(10*H*)-one was used without further purification.

n-Butyllithium (0.56 mL, 0.90 mmol, 1.6 M) in hexanes was added to a solution of 0.11 mL (0.92 mmol) of 1-bromo-4-methoxybenzene in 2 mL of dry THF, and the mixture was stirred vigorously for 1 h. 10-Hydroxy-2-methyl-10-(phenylethynyl)anthra[2,3-*b*]thiophene-5-(10*H*)-one (0.090 g, 0.24 mmol) was dissolved in 3 mL of dry THF in a separate flask and cooled to −78 °C followed by the addition of the aryllithium suspension, and the reaction mixture was stirred overnight while slowly warming to room temperature. Then the reaction mixture was treated with 20 mL of 10% HCl aqueous solution saturated with tin(II) chloride dihydrate, extracted with CH_2Cl_2, and dried over $MgSO_4$. The crude **AE-AMT** was purified by flash chromatography on silica gel using CH_2Cl_2/hexanes (1:2, v/v) and then recrystallized from CH_2Cl_2 and hexanes to yield **AE-AMT** (0.05 g, 43%). Mp: >260 °C. ^{1}H NMR (500 MHz, $CDCl_3$): δ 9.12 (s, 1H), 9.00 (s, 1H), 8.73 (d, J = 8.7 Hz, 2H), 8.09 (s, 1H), 7.97 (s, 1H), 7.85−7.83 (m, 4H), 7.71 (d, J = 8.8 Hz, 2H), 7.57−7.54 (m, 2H), 7.51−7.47 (m, 4H), 7.46−7.43 (m, 2H), 7.39 (d, J = 8.6 Hz, 4H), 7.37−7.34 (m, 2H), 7.17 (d, J = 8.2 Hz, 4H), 7.14 (s, 1H), 6.92 (s, 1H), 3.99 (s, 6H), 2.624, 2.622 (s, 3H), 2.603, 2.601 (s, 3H). ^{13}C NMR (125 MHz, $CDCl_3$): δ 159.4, 159.3, 159.2, 144.6, 143.8, 143.6, 141.0, 140.5, 140.3, 140.0, 139.4, 138.8, 138.4, 137.4, 136.7, 135.6, 132.68, 132.66, 132.53, 132.51, 132.2, 132.1, 131.9, 131.8, 131.7, 131.1, 131.0, 130.4, 129.9, 129.8, 129.6, 128.8, 128.7, 128.59, 128.56, 128.3, 127.6, 127.5, 127.2, 127.05, 126.95, 126.1, 126.07, 125.1, 124.6, 124.55, 124.0, 123.9, 121.25, 121.22, 121.2, 120.0, 119.7, 119.4, 119.2, 119.1, 118.9, 116.9, 116.0, 114.12, 114.07, 101.3, 101.0, 87.3, 87.1, 55.6, 17.1, 17.0. HRMS (DART): calcd for $C_{32}H_{23}OS$ $(M + H)^+$ 455.1464, found 455.1488.

5,10-Bis((4-methoxyphenyl)ethynyl)-2-methylanthra[2,3-*b*]-thiophene (DE-AMT). *n*-Butyllithium (1.71 mL, 2.7 mmol, 1.6 M) in hexanes was added to a solution of 0.38 g (2.8 mmol) of 1-ethynyl-4-methoxybenzene in 8 mL of dry THF at −78 °C and stirred vigorously for 20 min, followed by the addition of 0.20 g (0.72 mmol) of **AMT quinone**. The reaction mixture was then allowed to slowly warm to room temperature overnight before treatment with 30 mL of 10% HCl aqueous solution saturated with tin(II) chloride dihydrate and extracted with CH_2Cl_2. The crude product was purified by flash chromatography on silica gel (CH_2Cl_2/hexanes, 1:1 v/v) and recrystallized from CH_2Cl_2 and hexanes to yield **DE-AMT** (0.18 g, 48%). Mp: 247.5−249.5 °C. ^{1}H NMR (500 MHz, $CDCl_3$): δ 9.08 (s, 1H), 8.95 (s, 1H), 8.70−8.68 (m, 2H), 7.77−7.75 (m, 4H), 7.60−7.58 (m, 2H), 7.16 (s, 1H), 7.02 (d, J = 8.6 Hz, 4H), 3.91 (s, 6H), 2.67 (s, 3H). ^{13}C NMR (125 MHz, $CDCl_3$): δ 160.13, 160.12, 144.6, 141.3, 140.5, 133.4, 133.3, 131.77, 131.75, 130.0, 129.4, 127.5, 127.4, 126.4, 121.3, 119.7, 119.5, 118.3, 117.4, 115.9, 115.8, 114.3, 102.8, 102.6, 86.0, 85.9, 55.6, 17.1. HRMS (DART): calcd for $C_{35}H_{25}O_2S$ $(M + H)^+$ 509.1570, found 509.1558.

5,11-Bis(4-methoxyphenyl)-2,8-dimethylanthra[2,3-*b*:6,7-*b*′]dithiophene (DA-ADT). *n*-Butyllithium (1.68 mL, 2.7 mmol, 1.6 M) in hexanes was added to a solution of 0.35 mL (2.8 mmol) of 1-bromo-4-methoxybenzene in 10 mL of dry THF at −78 °C and stirred vigorously for 30 min, followed by the addition of 0.24 g (0.69 mmol) of **ADT quinone**. The reaction mixture was then allowed to slowly warm to room temperature overnight before addition of 35 mL of 10% HCl aqueous solution saturated with tin(II) chloride dihydrate and extracted with CH_2Cl_2. The crude product was purified by flash chromatography on silica gel (CH_2Cl_2/hexanes, 1:1, v/v) and recrystallized from CH_2Cl_2 and hexanes to yield **DA-ADT** (0.18 g, 48%). Mp: >260 °C. ^{1}H NMR (500 MHz, $CDCl_3$): δ 8.066, 8.064 (s, 2H), 7.95 (s, 2H), 7.46 (d, J = 8.5 Hz, 4H), 7.22 (d, J = 8.6 Hz, 4H), 6.85 (s, 2H), 4.02 (s, 6H), 2.538, 2.536 (two singlets, 6H). ^{13}C NMR (125 MHz, $CDCl_3$): δ 159.19, 159.15, 159.1, 143.4, 143.3, 1139.68, 139.66, 138.40, 138.35, 136.4, 135.3, 134.2, 132.81, 132.78, 132.75, 131.9, 131.8, 128.3, 128.2, 127.9, 127.8, 121.1, 119.2, 119.1, 118.8, 118.7, 114.22, 114.17, 114.1, 55.5, 17.0. HRMS (DART): calcd for $C_{34}H_{27}O_2S_2$ $(M + H)^+$ 531.1447, found 531.1465.

5-(4-Methoxyphenyl)-2,8-dimethyl-11-(phenylethynyl)-anthrax[2,3-*b*:6,7-*b*′]dithiophene (AE-ADT). *n*-Butyllithium (0.34 mL, 0.55 mmol, 1.6 M) in hexanes was added to solution of 0.06 mL (0.57 mmol) of phenylacetylene in 2 mL of dry THF slowly at −78 °C, and the mixture was stirred vigorously for 45 min. The reaction mixture was slowly added to a solution of 0.20 g (0.57 mmol) of **ADT quinone** in 2 mL of dry THF at −78 °C. The solution was then allowed to slowly warm to room temperature and stirred overnight. The reaction mixture was filtered, and the solid in the filter was washed with 5 mL of THF/H_2O (1:1 v/v). The filtrate was mixed with NH_4Cl saturated aqueous solution and vigorously stirred for 30 min. The suspension was then extracted with CH_2Cl_2 and dried over $MgSO_4$. The crude 10-hydroxy-2-methyl-10-(phenylethynyl)anthra[2,3-*b*]-thiophene-5(10*H*)-one was used without further purification.

n-Butyllithium (0.79 mL, 1.3 mmol, 1.6 M) in hexanes was added to a solution of 0.24 mL (1.3 mmol) of 1-bromo-4-methoxybenzene in 2 mL of dry THF, and the mixture was stirred vigorously for 1 h. 11-Hydroxy-2,8-dimethyl-11-(phenylethynyl)anthra[2,3-*b*:6,7-*b*′]-dithiophene-5(11*H*)-one (0.20 g, 0.57 mmol) was dissolved in 2 mL of dry THF in a separate flask and cooled to −78 °C followed by the addition of the aryllithium suspension. The reaction mixture was stirred overnight while slowly warming to room temperature. Twenty milliliters of 10% HCl aqueous solution saturated with tin(II) chloride dihydrate was then added. The product was extracted with CH_2Cl_2 and dried over $MgSO_4$. The crude **AE-ADT** was purified by flash chromatography on silica gel using CH_2Cl_2/hexanes (1:2, v/v) and then recrystallized from CH_2Cl_2 and hexanes to yield **AE-ADT** (0.060 g, 32%). Mp: >260 °C. ^{1}H NMR (500 MHz, $CDCl_3$): δ 9.10 (s, 1H), 8.98 (s, 1H), 8.05 (s, 1H), 7.94 (s, 1H), 7.88−7.86 (m, 2H), 7.51 (t, J

dx.doi.org/10.1021/jo501696d | *J. Org. Chem.* 2014, 79, 10081−10093

= 7.6 Hz, 2H), 7.47−7.45 (m, 1H), 7.41 (d, J = 8.5 Hz, 2H), 7.19 (d, J = 8.4 Hz, 2H), 7.10 (s, 1H), 6.88 (s, 1H), 4.01 (s, 3H), 2.60 (s, 3H), 2.58 (s, 3H). ^{13}C NMR (125 MHz, $CDCl_3$): δ 159.3, 144.5, 144.4, 143.6, 143.5, 140.83, 140.81, 140.2, 140.00, 139.95, 138.93, 138.89, 138.3, 137.3, 136.2, 132.63, 132.61, 132.6, 131.9, 131.82, 131.78, 131.4, 131.3, 130.17, 130.15, 129.7, 128.7, 128.53, 128.51, 128.2, 128.1, 127.8, 127.7, 124.0, 121.19, 121.17, 119.85, 119.75, 119.5, 119.4, 119.0, 118.9, 118.7, 118.6, 115.3, 114.3, 114.2, 114.13, 114.08, 101.3, 101.0, 87.6, 77.4, 77.1, 76.9, 55.5, 17.1, 17.0. HRMS (DART): calcd for $C_{35}H_{25}OS_2$ $(M + H)^+$ 525.1341, found 525.1323.

5,11-Bis((4-methoxyphenyl)ethynyl)-2,8-dimethylanthra[2,3-*b*:6,7-*b*′]dithiophene (DE-ADT). *n*-Butyllithium (1.56 mL, 2.5 mmol, 1.6 M) in hexanes was added to a solution of 0.35 g (2.6 mmol) of 1-ethynyl-4-methoxybenzene in 8 mL of dry THF at −78 °C, and the mixture was stirred vigorously for 20 min, followed by the addition of 0.30 g (0.86 mmol) of **ADT quinone**. The reaction mixture was then allowed to slowly warm to room temperature overnight before addition of 30 mL of 10% HCl aqueous solution saturated with tin(II) chloride dihydrate and extracted with CH_2Cl_2. The crude product was purified by flash chromatography on silica gel (CH_2Cl_2/hexanes, 1:1, v/v) and recrystallized from CH_2Cl_2 and hexanes to yield **DE-ADT** (0.23 g, 46%). Mp: >260 °C. ^{1}H NMR (500 MHz, $CDCl_3$): δ 9.06 (s, 2H), 8.93 (s, 2H), 7.80−7.77 (m, 4H), 7.12 (s, 2H), 7.04−7.02 (m, 4H), 3.91 (s, 6H), 2.65 (s, 6H). This compound was not sufficiently soluble for ^{13}C NMR spectroscopy. HRMS (DART): calcd for $C_{38}H_{27}O_2S_2$ $(M + H)^+$ 579.1447, found 579.1451.

2-Methyltetraceno[2,3-*b*]thiophene-5,12-dione (TMT quinone). 5-Methylthiophene-2,3-dicarbaldehyde (0.15 g, 1.0 mmol) and 0.21 g (1.0 mmol) of anthracene-1,4-diol[88] were dissolved in 5 mL of ethanol, and the mixture was vigorously stirred for 1 h at room temperature followed by the addition of 1 mL of 10% aqueous NaOH. After stirring at room temperature overnight, the reaction was filtered, and the solid in the filter was washed with 10 mL of deionized H_2O and 5 mL of acetone. The crude 2-methyltetraceno[2,3-*b*]thiophene-5,12-dione was used without purification to yield **TMT quinone** (0.30 g, 91%). Mp: >260 °C. ^{1}H NMR (500 MHz, $CDCl_3$): δ 8.91 (s, 2H), 8.82 (s, 1H), 8.68 (s, 1H), 8.13−8.11 (m, 2H), 7.72−7.70 (m, 2H), 7.26 (s, 1H), 2.70 (s, 3H). ^{13}C NMR (125 MHz, $CDCl_3$): δ 183.6, 183.1, 148.3, 145.3, 144.7, 135.5, 135.4, 131.0, 130.5, 130.3, 129.8, 129.6, 123.2, 122.5, 122.4, 16.8. HRMS (DART): calcd for $C_{21}H_{13}O_2S$ $(M + H)^+$ 329.0631, found 329.0633.

5,12-Bis(4-methoxyphenyl)-2-methyltetraceno[2,3-*b*]thiophene (DA-TMT). *n*-Butyllithium (0.67 mL, 1.1 mmol, 1.6 M) in hexanes was added to a solution of 0.14 mL (1.10 mmol) of 1-bromo-4-methoxybenzene in 3 mL of dry THF at −78 °C, and the mixture was stirred vigorously for 30 min, followed by the addition of 0.090 g (0.27 mmol) of **TMT quinone**. The reaction mixture was then allowed to slowly warm to room temperature overnight before addition of 20 mL of 10% HCl aqueous solution saturated with tin(II) chloride dehydrate. After extraction with CH_2Cl_2, the crude product was purified by flash chromatography on silica gel (CH_2Cl_2/hexanes, 1:1, v/v) and recrystallized from CH_2Cl_2 and hexanes to yield **DA-TMT** (0.060 g, 41%). Mp: >260 °C. ^{1}H NMR (500 MHz, $CDCl_3$): δ 8.34 (s, 2H), 8.08 (s, 1H), 7.97 (s, 1H), 7.79−7.77 (m, 2H), 7.51 (d, J = 8.6 Hz, 4H), 7.28−7.24 (m, 6H), 6.84 (s, 1H), 4.04 (s, 6H), 2.535, 2.533 (s, 3H). ^{13}C NMR (125 MHz, $CDCl_3$): δ 159.4, 159.3, 143.9, 140.2, 138.8, 136.6, 135.4, 133.01, 132.98, 132.1, 131.9, 130.94, 130.92, 129.2, 12.1, 128.68, 128.67, 128.65, 128.2, 125.8, 125.7, 125.12, 125.10, 121.1, 119.3, 118.9, 114.4, 114.3, 55.7, 17.1. HRMS (DART): calcd for $C_{35}H_{27}O_2S$ $(M + H)^+$ 511.1726, found 511.1723.

12-(4-Methoxyphenyl)-2-methyl-5-(phenylethynyl)tetraceno[2,3-*b*]thiophene (AE-TMT). *n*-Butyllithium (0.38 mL, 0.61 mmol, 1.6 M) in hexanes was added to solution of 0.070 mL (0.61 mmol) of phenylacetylene in 2.5 mL of dry THF slowly at −78 °C and stirred vigorously for 45 min. The reaction mixture was slowly added to a solution of 0.20 g (0.61 mmol) of **TMT quinone** in 4 mL of dry THF at −78 °C. The solution was then allowed to slowly warm to room temperature and stirred overnight. The reaction mixture was filtered, and the solid in the filter was washed with 10 mL of THF/H_2O (1:1, v/v). The filtrate was mixed with NH_4Cl saturated aqueous solution, and the mixture was vigorously stirred for 30 min. The suspension was then extracted with CH_2Cl_2 and dried over $MgSO_4$. The crude 5-hydroxy-2-methyl-5-(phenylethynyl)tetracene[2,3-*b*]-thiophen-12(5*H*)-one was used without further purification.

n-Butyllithium (0.33 mL, 0.53 mmol, 1.6 M) in hexanes was added to a solution of 0.07 mL (0.54 mmol) of 1-bromo-4-methoxybenzene in 2 mL of dry THF, and the mixture was stirred vigorously for 1 h. 5-Hydroxy-2-methyl-5-(phenylethynyl)tetracene[2,3-*b*]thiophen-12(5*H*)-one (0.060 g, 0.14 mmol) was dissolved in 2 mL of dry THF in a separate flask and cooled to −78 °C followed by the addition of the aryllithium suspension, and the reaction mixture was stirred overnight while slowly warming to room temperature. Then the reaction mixture was treated with 20 mL of 10% HCl aqueous solution saturated with tin(II) chloride dihydrate, extracted with CH_2Cl_2, and dried over $MgSO_4$. The crude **AE-TMT** was purified by flash chromatography on silica gel using CH_2Cl_2/hexanes (1:2, v/v) and then recrystallized from CH_2Cl_2 and hexanes to yield **AE-TMT** (0.040 g, 53%). Mp: >260 °C. ^{1}H NMR (500 MHz, $CDCl_3$): δ 9.34 (s, 2H), 9.10 (s, 1H), 8.98 (s, 1H), 8.33 (s, 2H), 8.09 (s, 3H), 7.96 (s, 1H), 7.92−7.90 (m, 4H), 7.81 (d, J = 8.5 Hz, 2H), 7.53 (t, J = 7.6 Hz, 4H), 7.48−7.45 (m, 6H), 7.40 (t, J = 7.4 Hz, 2H), 7.33 (t, J = 7.4 Hz, 2H), 7.22 (d, J = 8.3 Hz, 4H), 7.09 (s, 1H), 6.87 (s, 1H), 4.03 (s, 6H), 2.60 (s, 3H), 2.58 (3H). ^{13}C NMR (125 MHz, $CDCl_3$): δ 159.5, 144.1, 139.4, 132.84, 138.82, 132.0, 131.9, 131.8, 131.4, 130.4, 128.8, 126.7, 126.6, 125.9, 125.5, 125.4, 121.30, 121.27, 119.9, 119.6, 119.2, 118.9, 114.3, 114.2, 55.7, 17.3, 17.2. HRMS (DART): calcd for $C_{36}H_{25}OS$ $(M + H)^+$ 505.1621, found 505.1627.

5,12-Bis((4-methoxyphenyl)ethynyl)-2-methyltetraceno[2,3-*b*]thiophene (DE-TMT). *n*-Butyllithium (0.55 mL, 0.88 mmol, 1.6 M) in hexanes was added to a solution of 0.12 g (0.91 mmol) of 1-ethynyl-4-methoxybenzene in 7 mL of dry THF at −78 °C, and the mixture was stirred vigorously for 20 min, followed by the addition of 0.10 g (0.30 mmol) of **TMT quinone**. The reaction mixture was then allowed to slowly warm to room temperature overnight before treatment with 20 mL of 10% HCl aqueous solution saturated with tin(II) chloride dihydrate and extracted with CH_2Cl_2. The crude product was purified by flash chromatography on silica gel (CH_2Cl_2/hexanes, 1:1, v/v) and recrystallized from CH_2Cl_2 and hexanes to yield **DE-TMT** (0.060 g, 37%). Mp: >260 °C. ^{1}H NMR (500 MHz, $CDCl_3$): δ 9.30 (s, 2H), 9.06 (s, 1H), 8.94 (s, 1H), 8.10−8.08 (m, 2H), 7.83−7.82 (m, 4H), 7.46−7.44 (m, 2H), 7.11 (s, 1H), 7.06 (d, J = 8.8 Hz, 4H), 3.93 (s, 6H), 2.65 (s, 3H). **DE-TMT** was not soluble enough for high quality ^{13}C NMR. Reported here are the resonances we could identify. ^{13}C NMR (125 MHz, $CDCl_3$): δ 160.3, 144.9, 141.6, 133.51, 133.46, 132.2, 130.5, 130.0, 128.8, 126.2, 126.1, 126.0, 121.4, 119.7, 119.5, 116.0, 114.6, 104.0, 103.7, 86.8, 86.7, 55.7, 17.3. HRMS (DART): calcd for $C_{39}H_{27}O_2S$ $(M + H)^+$ 559.1726, found 559.1724.

■ ASSOCIATED CONTENT

Supporting Information

NMR spectra of all previously unreported acenes and heteroacenes, pseudo-first-order kinetics plots for reactions with singlet oxygen, cyclic voltammograms, and atomic coordinates and total energies for optimized geometries determined using DFT calculations. This material is available free of charge via the Internet at http://pubs.acs.org.

■ AUTHOR INFORMATION

Corresponding Author

*E-mail: sam.thomas@tufts.edu. Tel: 1-617-627-3771.

Notes

The authors declare no competing financial interest.

■ ACKNOWLEDGMENTS

This work was supported by the National Science Foundation (Grant CHE-1305832). We thank Prof. Elena Rybak-Akimova for assistance with cyclic voltammetry measurements.

■ REFERENCES

(1) Anthony, J. E. *Chem. Rev.* **2006**, *106*, 5028−5048.
(2) Wang, C.; Dong, H.; Hu, W.; Liu, Y.; Zhu, D. *Chem. Rev.* **2012**, *112*, 2208−2267.
(3) Allard, S.; Forster, M.; Souharce, B.; Thiem, H.; Scherf, U. *Angew. Chem., Int. Ed.* **2008**, *47*, 4070−4098.
(4) Anthony, J. E. *Angew. Chem., Int. Ed.* **2008**, *47*, 452−483.
(5) Spanggaard, H.; Krebs, F. C. *Sol. Energy Mater. Sol. Cells* **2004**, *83*, 125−146.
(6) Smith, M. B.; Michl, J. *Chem. Rev.* **2010**, *110*, 6891−6936.
(7) Zehm, D.; Fudickar, W.; Hans, M.; Schilde, U.; Kelling, A.; Linker, T. *Chem.—Eur. J.* **2008**, *14*, 11429−11441.
(8) Fudickar, W.; Linker, T. *Chem. Commun.* **2008**, 1771−1773.
(9) Allen, C. F. H.; Bell, A. *J. Am. Chem. Soc.* **1942**, *64*, 1253−1260.
(10) Fudickar, W.; Fery, A.; Linker, T. *J. Am. Chem. Soc.* **2005**, *127*, 9386−9387.
(11) Miao, Q.; Chi, X.; Xiao, S.; Zeis, R.; Lefenfeld, M.; Siegrist, T.; Steigerwald, M. L.; Nuckolls, C. *J. Am. Chem. Soc.* **2006**, *128*, 1340−1345.
(12) Kaur, I.; Miller, G. P. *New J. Chem.* **2008**, *32*, 459−463.
(13) Jang, B. B.; Lee, S. H.; Kafafi, Z. H. *Chem. Mater.* **2006**, *18*, 449−457.
(14) Kaur, I.; Jia, W.; Kopreski, R. P.; Selvarasah, S.; Dokmeci, M. R.; Pramanik, C.; McGruer, N. E.; Miller, G. P. *J. Am. Chem. Soc.* **2008**, *130*, 16274−16286.
(15) Kaur, I.; Stein, N. N.; Kopreski, R. P.; Miller, G. P. *J. Am. Chem. Soc.* **2009**, *131*, 3424−3425.
(16) Anthony, J. E.; Brooks, J. S.; Eaton, D. L.; Parkin, S. R. *J. Am. Chem. Soc.* **2001**, *123*, 9482−9483.
(17) Payne, M. M.; Odom, S. A.; Parkin, S. R.; Anthony, J. E. *Org. Lett.* **2004**, *6*, 3325−3328.
(18) Payne, M. M.; Parkin, S. R.; Anthony, J. E. *J. Am. Chem. Soc.* **2005**, *127*, 8028−8029.
(19) Purushothaman, B.; Parkin, S. R.; Anthony, J. E. *Org. Lett.* **2010**, *12*, 2060−2063.
(20) Purushothaman, B.; Bruzek, M.; Parkin, S. R.; Miller, A. F.; Anthony, J. E. *Angew. Chem., Int. Ed.* **2011**, *50*, 7013−7017.
(21) Jiang, W.; Li, Y.; Wang, Z. *Chem. Soc. Rev.* **2013**, *42*, 6113−6127.
(22) Bunz, U. H. F.; Engelhart, J. U.; Lindner, B. D.; Schaffroth, M. *Angew. Chem., Int. Ed.* **2013**, *52*, 3810−3821.
(23) Takimiya, K.; Shinamura, S.; Osaka, I.; Miyazaki, E. *Adv. Mater.* **2011**, *23*, 4347−4370.
(24) Tang, M. L.; Bao, Z. A. *Chem. Mater.* **2011**, *23*, 446−455.
(25) Lim, Y. F.; Shu, Y.; Parkin, S. R.; Anthony, J. E.; Malliaras, G. G. *J. Mater. Chem.* **2009**, *19*, 3049−3056.
(26) Lehnherr, D.; Tykwinski, R. R. *Aust. J. Chem.* **2011**, *64*, 919−929.
(27) Atherton, J. C. C.; Jones, S. *Tetrahedron* **2003**, *59*, 9039−9057.
(28) Watanabe, M.; Chen, K.-Y.; Chang, Y. J.; Chow, T. J. *Acc. Chem. Res.* **2013**, *46*, 1606−1615.
(29) Gacal, B.; Durmaz, H.; Tasdelen, M. A.; Hizal, G.; Tunca, U.; Yagci, Y.; Demirel, A. L. *Macromolecules* **2006**, *39*, 5330−5336.
(30) Ishow, E.; Bouffard, J.; Kim, Y.; Swager, T. M. *Macromolecules* **2006**, *39*, 7854−7858.
(31) Yoshie, N.; Saito, S.; Oya, N. *Polymer* **2011**, *52*, 6074−6079.
(32) Klanderman, B. H.; Criswell, T. R. *J. Org. Chem.* **1969**, *34*, 3426−3430.
(33) Friedman, L.; Logullo, F. M. *J. Am. Chem. Soc.* **1963**, *85*, 1549.
(34) Gidron, O.; Shimon, L. J. W.; Leitus, G.; Bendikov, M. *Org. Lett.* **2012**, *14*, 502−505.
(35) Zade, S. S.; Bendikov, M. *J. Phys. Org. Chem.* **2012**, *25*, 452−461.
(36) Schleyer, P. V.; Manoharan, M.; Jiao, H. J.; Stahl, F. *Org. Lett.* **2001**, *3*, 3643−3646.
(37) Aubry, J.-M.; Pierlot, C.; Rigaudy, J.; Schmidt, R. *Acc. Chem. Res.* **2003**, *36*, 668−675.
(38) Turro, N. J.; Ramamurthy, V.; Scaiano, J. C. *Modern Molecular Photochemistry of Organic Molecules*; University Science Books: Sausalito, CA, 2010.
(39) Fudickar, W.; Linker, T. *J. Am. Chem. Soc.* **2012**, *134*, 15071−15082.
(40) Maliakal, A.; Raghavachari, K.; Katz, H.; Chandross, E.; Siegrist, T. *Chem. Mater.* **2004**, *16*, 4980−4986.
(41) Dolmans, D. E. J. G. J.; Fukumura, D.; Jain, R. K. *Nat. Rev. Cancer* **2003**, *3*, 380−387.
(42) Clennan, E. L.; Pace, A. *Tetrahedron* **2005**, *61*, 6665−6691.
(43) Hoffmann, N. *Chem. Rev.* **2008**, *108*, 1052−1103.
(44) Umezawa, N.; Tanaka, K.; Urano, Y.; Kikuchi, K.; Higuchi, T.; Nagano, T. *Angew. Chem., Int. Ed.* **1999**, *38*, 2899−2901.
(45) Tanaka, K.; Miura, T.; Umezawa, N.; Urano, Y.; Kikuchi, K.; Higuchi, T.; Nagano, T. *J. Am. Chem. Soc.* **2001**, *123*, 2530−2536.
(46) Miura, T.; Urano, Y.; Tanaka, K.; Nagano, T.; Ohkubo, K.; Fukuzumi, S. *J. Am. Chem. Soc.* **2003**, *125*, 8666−8671.
(47) Cao, Y. F.; Koo, Y. E. L.; Koo, S. M.; Kopelman, R. *Photochem. Photobiol.* **2005**, *81*, 1489−1498.
(48) Song, B.; Wang, G. L.; Tan, M. Q.; Yuan, J. L. *J. Am. Chem. Soc.* **2006**, *128*, 13442−13450.
(49) Liu, Y. J.; Wang, K. Z. *Eur. J. Inorg. Chem.* **2008**, 5214−5219.
(50) Koylu, D.; Sarrafpour, S.; Zhang, J.; Ramjattan, S.; Panzer, M. J.; Thomas, S. W. *Chem. Commun.* **2012**, *48*, 9489−9491.
(51) Zhang, J.; Sarrafpour, S.; Pawle, R. H.; Thomas, S. W. *Chem. Commun.* **2011**, *47*, 3445−3447.
(52) Dai, Z.; Tian, L.; Xiao, Y.; Ye, Z.; Zhang, R.; Yuan, J. *J. Mater. Chem. B* **2013**, *1*, 924−927.
(53) Fudickar, W.; Linker, T. *Chem.—Eur. J.* **2006**, *12*, 9276−9283.
(54) Ullman, E. F.; Kirakossian, H.; Singh, S.; Wu, Z. P.; Irvin, B. R.; Pease, J. S.; Switchenko, A. C.; Irvine, J. D.; Dafforn, A.; Skold, C. N.; Wagner, D. B. *Proc. Natl. Acad. Sci. U.S.A.* **1994**, *91*, 5426−5430.
(55) Bouas-Laurent, H.; Durr, H. *Pure Appl. Chem.* **2001**, *73*, 639−665.
(56) Zhang, J.; Sarrafpour, S.; Haas, T. E.; Müller, P.; Thomas, S. W. *J. Mater. Chem.* **2012**, *22*, 6182−6189.
(57) Anthony, J. E.; Eaton, D. L.; Parkin, S. R. *Org. Lett.* **2002**, *4*, 15−18.
(58) Griffith, O. L.; Anthony, J. E.; Jones, A. G.; Lichtenberger, D. L. *J. Am. Chem. Soc.* **2009**, *132*, 580−586.
(59) Park, S. K.; Jackson, T. N.; Anthony, J. E.; Mourey, D. A. *Appl. Phys. Lett.* **2007**, *91*, No. 063514.
(60) Fudickar, W.; Linker, T. *Chem.—Eur. J.* **2011**, *17*, 13661−13664.
(61) Zhang, J.; Pawle, R. H.; Haas, T. E.; Thomas, S. W. *Chem.—Eur. J.* **2014**, *20*, 5880−5884.
(62) Etschel, S. H.; Waterloo, A. R.; Margraf, J. T.; Amin, A. Y.; Hampel, F.; Jäger, C. M.; Clark, T.; Halik, M.; Tykwinski, R. R. *Chem. Commun.* **2013**, *49*, 6725−6727.
(63) Barlier, V. S.; Schlenker, C. W.; Chin, S. W.; Thompson, M. E. *Chem. Commun.* **2011**, *47*, 3754−3756.
(64) Zhang, X. J.; Jiang, X. X.; Luo, J.; Chi, C. Y.; Chen, H. Z.; Wu, J. S. *Chem.—Eur. J.* **2010**, *16*, 464−468.
(65) Tang, M. L.; Reichardt, A. D.; Okamoto, T.; Miyaki, N.; Bao, Z. A. *Adv. Funct. Mater.* **2008**, *18*, 1579−1585.
(66) Tang, M. L.; Okamoto, T.; Bao, Z. N. *J. Am. Chem. Soc.* **2006**, *128*, 16002−16003.
(67) Laquindanum, J. G.; Katz, H. E.; Lovinger, A. J. *J. Am. Chem. Soc.* **1998**, *120*, 664−672.
(68) Anthony, J. E.; Subramanian, S.; Parkin, S. R.; Park, S. K.; Jackson, T. N. *J. Mater. Chem.* **2009**, *19*, 7984−7989.
(69) Valiyev, F.; Hu, W. S.; Chen, H. Y.; Kuo, M. Y.; Chao, I.; Tao, Y. T. *Chem. Mater.* **2007**, *19*, 3018−3026.
(70) Balandier, J. Y.; Quist, F.; Sebaihi, N.; Niebel, C.; Tylleman, B.; Boudard, P.; Bouzakraoui, S.; Lemaur, V.; Cornil, J.; Lazzaroni, R.; Geerts, Y. H.; Stas, S. *Tetrahedron* **2011**, *67*, 7156−7161.

(71) Lehnherr, D.; Gao, J.; Hegmann, F. A.; Tykwinski, R. R. *Org. Lett.* **2008**, *10*, 4779−4782.
(72) Lehnherr, D.; McDonald, R.; Ferguson, M. J.; Tykwinski, R. R. *Tetrahedron* **2008**, *64*, 11449−11461.
(73) Lehnherr, D.; McDonald, R.; Tykwinski, R. R. *Org. Lett.* **2008**, *10*, 4163−4166.
(74) Lehnherr, D.; Waterloo, A. R.; Goetz, K. P.; Payne, M. M.; Hampel, F.; Anthony, J. E.; Jurchescu, O. D.; Tykwinski, R. R. *Org. Lett.* **2012**, *14*, 3660−3663.
(75) Mamada, M.; Minamiki, T.; Katagiri, H.; Tokito, S. *Org. Lett.* **2012**, *14*, 4062−4065.
(76) Tylleman, B.; Vande Velde, C. M. L.; Balandier, J. Y.; Stas, S.; Sergeyev, S.; Geerts, Y. H. *Org. Lett.* **2011**, *13*, 5208−5211.
(77) Northrop, B. H.; Houk, K. N.; Maliakal, A. *Photochem. Photobiol. Sci.* **2008**, *7*, 1463−1468.
(78) Kim, C.; Huang, P.-Y.; Jhuang, J.-W.; Chen, M.-C.; Ho, J.-C.; Hu, T.-S.; Yan, J.-Y.; Chen, L.-H.; Lee, G.-H.; Facchetti, A.; Marks, T. J. *Org. Electron.* **2010**, *11*, 1363−1375.
(79) Palayangoda, S. S.; Mondal, R.; Shah, B. K.; Neckers, D. C. *J. Org. Chem.* **2007**, *72*, 6584−6587.
(80) Peach, M. J. G.; Williamson, M. J.; Tozer, D. J. *J. Chem. Theory Comput.* **2011**, *7*, 3578−3585.
(81) Foote, C. S.; Chang, Y. C.; Denny, R. W. *J. Am. Chem. Soc.* **1970**, *92*, 5216−5218.
(82) Foote, C. S.; Chang, Y. C.; Denny, R. W. *J. Am. Chem. Soc.* **1970**, *92*, 5218−5219.
(83) Chun, D.; Cheng, Y.; Wudl, F. *Angew. Chem., Int. Ed.* **2008**, *47*, 8380−8385.
(84) Chen, M.-C.; Kim, C.; Chen, S.-Y.; Chiang, Y.-J.; Chung, M.-C.; Facchetti, A.; Marks, T. J. *J. Mater. Chem.* **2008**, *18*, 1029−1036.
(85) Lakowicz, J. *Principles of Fluorescence Spectroscopy*, 3rd ed.; Springer Publishing: New York, 2006.
(86) Drexhage, K. H. *J. Res. Natl. Bur. Stand., Sect. A* **1976**, *80*, 421−428.
(87) Frisch, M. J.; Trucks, G. W.; Schlegel, H. B.; Scuseria, G. E.; Robb, M. A.; Cheeseman, J. R.; Scalmani, G.; Barone, V.; Mennucci, B.; Petersson, G. A.; Nakatsuji, H.; Caricato, M.; Li, X.; Hratchian, H. P.; Izmaylov, A. F.; Bloino, J.; Zheng, G.; Sonnenberg, J. L.; Hada, M.; Ehara, M.; Toyota, K.; Fukuda, R.; Hasegawa, J.; Ishida, M.; Nakajima, T.; Honda, Y.; Kitao, O.; Nakai, H.; Vreven, T.; Montgomery, J. A., Jr.; Peralta, J. E.; Ogliaro, F.; Bearpark, M.; Heyd, J. J.; Brothers, E.; Kudin, K. N.; Staroverov, V. N.; Kobayashi, R.; Normand, J.; Raghavachari, K.; Rendell, A.; Burant, J. C.; Iyengar, S. S.; Tomasi, J.; Cossi, M.; Rega, N.; Millam, J. M.; Klene, M.; Knox, J. E.; Cross, J. B.; Bakken, V.; Adamo, C.; Jaramillo, J.; Gomperts, R.; Stratmann, R. E.; Yazyev, O.; Austin, A. J.; Cammi, R.; Pomelli, C.; Ochterski, J. W.; Martin, R. L.; Morokuma, K.; Zakrzewski, V. G.; Voth, G. A.; Salvador, P.; Dannenberg, J. J.; Dapprich, S.; Daniels, A. D.; Farkas, O.; Foresman, J. B.; Ortiz, J. V.; Cioslowski, J.; Fox, D. J. *Gaussian 09*, Revision D.01; Gaussian, Inc.: Wallingford, CT, 2009.
(88) Hua, D. H.; Tamura, M.; Huang, X.; Stephany, H. A.; Helfrich, B. A.; Perchellet, E. M.; Sperfslage, B. J.; Perchellet, J.-P.; Jiang, S.; Kyle, D. E.; Chiang, P. K. *J. Org. Chem.* **2002**, *67*, 2907−2912.